Effect of Polyoxyethylene (10) Octylphenyl Ether on the Solution Viscosity and Density in the Belousov-Zhabotinsky Reaction

Minoru Yoshimoto,[1] Shingo Kubo,[1] and Shigeru Kurosawa[2]

[1]*Department of Information Science and Biomedical Engineering, Graduate School of Science and Engineering, Kagoshima University, 1-21-40 Korimoto, Kagoshima 890-0065, Japan*

[2]*Research Institute for Environmental Management Technology, National Institute of Advanced Industrial Science and Technology (AIST), AIST Tsukuba West, 16-1 Onogawa, Tsukuba, Ibaraki 305-8569, Japan*

(Received January 31, 2013; Revised May 27, 2013)

We investigated the dynamical behavior between the redox potential and the viscosity and density of the Belousov-Zhabotinsky (BZ) reaction by the systematic variation of the mixing level and the solution viscosity and density. The mixing level was controlled by the stirrer bar speed, and the solution viscosity and density was changed by the addition of polyoxyethylene (10) octylphenyl ether (Triton X-100). This study has revealed that three types of oscillations with phase difference appear, depending on the mixing level and the solution viscosity and density of the BZ reaction. It has also become clear that the critical micellization concentration (cmc) plays an important role in the behavior of the oscillation of the solution viscosity and density.

DOI: 10.6122/CJP.52.215 PACS numbers: 05.45.-a, 82.40.Bj, 82.40.Ck, 47.54.-r

I. INTRODUCTION

The Belousov-Zhabotinsky (BZ) reaction is well-known as one of the most famous oscillating chemical reactions. The BZ reaction exhibits a wide variety of nonlinear phenomena, e.g., target pattern or spiral pattern in an unstirred shallow solution and multistability, periodicity, multiperiodicity, or deterministic chaos in a stirred solution [1–3].

The chemical wave in the unstirred shallow solution of the BZ reaction has features that differ significantly from the familiar reaction-diffusion wave, because the convective mass transport plays a relevant role. The effects of convection on the propagation of the chemical wave have been observed experimentally [4–6]. The convection enhances the chemical wave speed and affects the curvature of the wave front. The natural convection disturbs a traveling wave, and the disturbed wave affects a convection pattern. This hydrodynamical effect is strongly affected by the solution viscosity and density. Recently, it has been reported that, in the unstirred batch system, the solution viscosity and density of the BZ reaction behaved as a bifurcation parameter for the sequence chaos $\rightarrow$ quasi-periodicity $\rightarrow$ period-1 and, in the stirred batch system, affected the oscillation period and the duration of the rising portion of the oscillatory cycle [7–9]. It is obvious that the solution viscosity and density of the BZ reaction plays an important role in the spatial and temporal patterns.

On the other hand, the mixing effects on the BZ reaction have been reported [10–12]. These effects include the changes in both the frequency and the amplitude of oscillation

and the quenching of spontaneous oscillation. The mixing also plays an important role in the BZ reaction.

In the previous studies, the oscillation of the BZ reaction has been monitored only by the change of the redox potential and the absorbance. On the other hand, in our recent paper [13], we have reported that the quartz crystal microbalance (QCM) was able to directly measure the dynamic behavior of the solution viscosity and density of the BZ reaction, $\sqrt{\rho_L \eta_L}$ (ρ_L and η_L are the absolute viscosity and the density of a solution, respectively) [14, 15]. However, the dynamic behavior between the redox potential and the solution viscosity and density of the BZ reaction is still not revealed in detail. Therefore, in this paper, we investigate its dynamic behavior by the systematic variation of the mixing level and the solution viscosity and density. Especially, we focus our aim on the phase difference between the redox potential and the solution viscosity and density.

II. EXPERIMENT

Malonic acid (MA), $NaBrO_3$, H_2SO_4, $FeSO_4 \cdot 7H_2O$, KBr (WAKO Pure Chemical Industries, Ltd., Japan) and O-phenanthroline·H_2O (DOJINDO, Japan) were of commercial analytical grade and were used without further purification. The solution of $[Fe(Phen)_3]^{2+}$, ferroin, was prepared by dissolving $FeSO_4 \cdot 7H_2O$ and O-phenanthroline·H_2O in pure water with the specific resistance of 18.2 M·cm. Water was purified by the Milli-Q apparatus (Millipore, Japan) and was deaerated before the experiments. In the present experiments, we employed the system of [MA] = 0.29 M, [$NaBrO_3$] = 0.28 M, [ferroin] = 0.69 mM, [H_2SO_4] = 0.57 M, and [KBr] = 0.067M.

The schematic diagram of the experimental setup is illustrated in Figure 1(a). The BZ reaction was performed using a 30 ml solution in the batch reactor (31 mm in diameter and 46 mm in depth). The batch reactor was covered with a water jacket. The temperatures were kept at 25 ± 0.1 °C. The redox potential of the BZ reaction (E) was measured between the platinum electrode and the Ag | AgCl electrode (HORIBA 2060A-10T, Japan), using a K_2SO_4 salt bridge. The Pt and Ag | AgCl electrodes were connected to the IBM-compatible PC through the voltage follower.

In the case of the BZ reaction, the resonant-frequency shift of the QCM (ΔF) is mainly generated by the viscous penetration depth generated on the oscillating QCM, that is, $\sqrt{\rho_L \eta_L}$ [11, 12]. In order to monitor $\sqrt{\rho_L \eta_L}$ of the BZ reaction, the 9 MHz AT-cut QCM (SEIKO EG & G, Ltd., Japan) was employed. The DCM had the configuration of the round quartz crystal of 8 mm diameter and a pair of round platinum electrodes of 5 mm diameter (Fig. 1(b)). The QCM was connected into a series resonant TTL circuit (SEIKO EG&G QCA917-21, Japan), which caused the QCM to oscillate at a resonant frequency near 9 MHz. The TTL circuit was powered from a 5 V dc supply. The resonant-frequency shift was monitored by a universal frequency counter (Agilent technologies 53131A) connected to the PC measuring the redox potential. The sampling times of both the redox potential and the resonant frequency were set at 0.1 s.

In the present experiments, one side of the QCM was sealed with a blank quartz

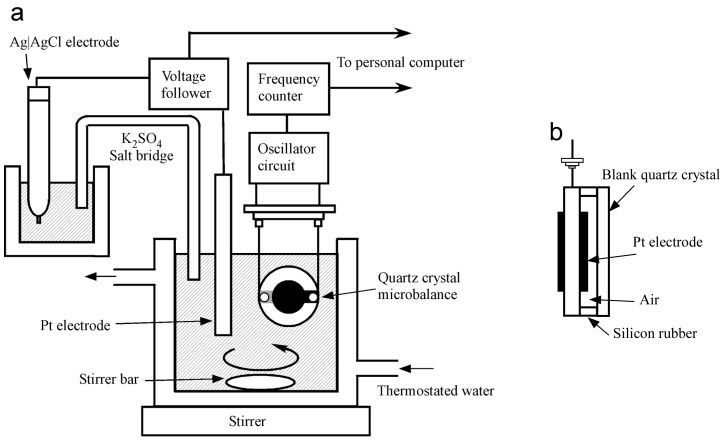

FIG. 1: (a) Schematic illustration of the experimental setup. The Pt and Ag | AgCl electrodes, and the quartz crystal microbalance (QCM) were used to measure the redox potential and the solution viscosity and density of the BZ reaction, respectively. (b) Schematic diagram of the one-face sealed QCM.

crystal casing (Fig. 1(b)), maintaining it in an air environment, while the other side was in contact with the solution of the BZ reaction. This casing is essential for the frequency stability of the QCM in an ionic solution [16]. The one-face sealed QCM was vertically immersed into the solution of the BZ reaction (Figure 1(a)).

The mixing levels of the solution of the BZ reaction were controlled using the stirrer bar (20 mm in length and 5 mm in diameter) and the magnetic stirrer (AS ONE ML-101, Japan). The solution viscosity and density of the BZ reaction was varied using polyoxyethylene (10) octylphenyl ether (Triton X-100) (WAKO Pure Chemical Industries, Ltd., Japan), which was added in preparation of the solution of the BZ reaction.

III. FERROIN/FERRIIN CATALYZED BZ REACTION

The mechanism of the ferroin/ferriin catalyzed BZ reaction is described as a cycle of three processes [17, 18].

Process A: Removal of the inhibitory species Br^-.

$$BrO_3^- + Br^- + 2H^+ \rightarrow HBrO_2 + HOBr, \qquad k_1 = 1.2\ M^{-3}s^{-1}, \tag{R1}$$

$$HBrO_2 + Br^- + H^+ \rightarrow 2HOBr, \qquad k_2 = 2.5 \times 10^6\ M^{-2}s^{-1}, \tag{R2}$$

$$HOBr + Br^- + H^+ \rightarrow Br_2 + H_2O, \qquad k_3 = 8 \times 10^9\ M^{-2}s^{-1}. \tag{R3}$$

Process B: Autocatalytic production of $HBrO_3$.

$$BrO_3^- + HBrO_2 + H^+ \rightarrow 2BrO_2^{\cdot} + H_2O, \qquad k_4 = 42\ M^{-2}s^{-1}, \tag{R4}$$

$$\mathrm{BrO_2^{\cdot}} + \mathrm{Fe(phen)_3}^{2+} + \mathrm{H^+} \rightarrow \mathrm{HBrO_2} + \mathrm{Fe(phen)_3}^{3+}, \quad k_5 = 1 \times 10^9\ \mathrm{M^{-2}s^{-1}}, \quad \text{(R5)}$$

$$2\mathrm{HBrO_2} \rightarrow \mathrm{BrO_3^-} + \mathrm{HOBr} + \mathrm{H^+}, \qquad k_6 = 3.0 \times 10^3\ \mathrm{M^{-1}s^{-1}}. \quad \text{(R6)}$$

Process C: Reduction of the oxidized catalyst, reorganization of $\mathrm{Br^-}$, and removal of $\mathrm{HBrO_2}$.

$$\mathrm{Fe(phen)_3}^{3+} + \mathrm{BrMA} \rightarrow \mathrm{Fe(phen)_3}^{2+} + f\mathrm{Br^-} + \text{organic products}, \quad K_7 = 11.7\ \mathrm{M^{-1}s^{-1}}. \quad \text{(R7)}$$

Process C includes the stoichiometric and potential bifurcation factor f. Unlike cerium, ferriin cannot oxidize MA due to its relatively low redox potential.

The oscillation of the redox potential of the BZ reaction is caused by ferroin/ferriin in Eq. (7), i.e., the concentration oscillation between ferroin and ferriin. In a previous paper [13], we suggested that the main factor of ΔF is the viscosity variation of the BZ solution due to the rearrangement of water molecules surrounding ferroin/ferriin.

IV. RESULTS AND DISCUSSION

IV-1. Time series of ΔE and ΔF

In order to investigate in detail the dynamical behavior between the redox potential and the solution viscosity and density, we systematically varied the stirrer bar speed and the solution viscosity and density. Figure 2 shows the time series of ΔE and ΔF and the ΔE-ΔF phase portraits. It is obvious that ΔF changes in a rhythmic manner and is synchronized with the oscillation of ΔE in an anti-phase mode: when ΔE is high (the ratio of ferriin to ferroin is high), ΔF is low. We have found that there are typically three types of the oscillations with the phase difference appear depending on the stirrer speed and the solution viscosity and density. That is,

Type-I: The oscillation phase of ΔE is advanced for that of ΔF (Figs. 2(a) and 2(d)),

Type-II: The oscillation phase of both ΔE and ΔF is the same (Figs. 2(b) and 2(e)),

Type-III: The oscillation phase of ΔF is advanced for that of ΔE (Figs. 2(c) and 2(f)).

In these cases, when the phase difference time (τ) is $-1s \leq \tau \leq +1s$ the phases of both are the same, when $\tau < -1s$ the oscillation phase of ΔE is advanced, and when $\tau > +1s$ the oscillation phase of ΔF is advanced, where $\tau = t_E - t_F$ (t_E and t_F are the times of the rising points of the oscillations of ΔE and ΔF, respectively. See Fig. 2(c)). Here, we employ the average values calculated from 10 oscillations.

Generally, when the QCM is dipped into a solution, its resonant-frequency shift depends on $\sqrt{\rho_L \eta_L}$. The relationship between the resonant-frequency shift of the one-face sealed QCM and $\sqrt{\rho_L \eta_L}$ is described by the following equation [14]:

$$\Delta f = -\frac{f_0^{\frac{3}{2}}}{\sqrt{\pi \rho \mu}} \sqrt{\rho_L \eta_L}, \quad (1)$$

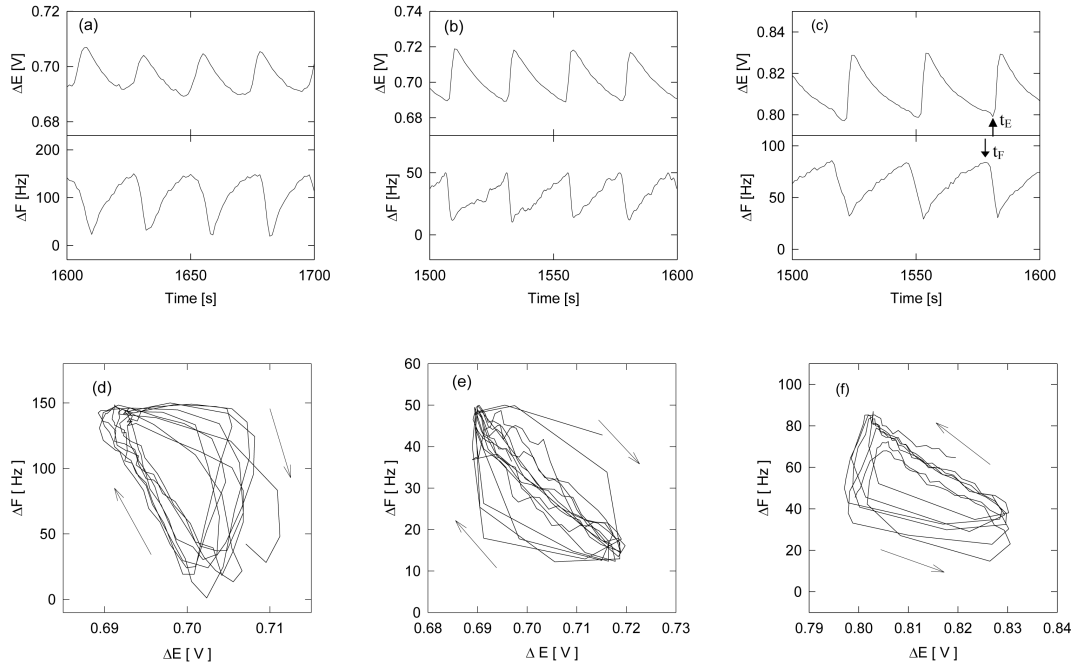

FIG. 2: Time series and phase portraits of the BZ reaction. (a), (b), and (c) are the time series of ΔE and ΔF. (d), (e), and (f) are the phase portraits composed from the time series of (a), (b), and (c), respectively. (a) and (d): the oscillation phase of the redox potential is advanced for that of ΔF (the stirrer bar speed is 50 rpm and the concentration of Triton-X is 0.020 wt%). (b) and (e): the oscillation phases of both ΔE and ΔF are almost equal (150 rpm and 0.010 wt%). (c) and (f): the oscillation phase of ΔF is advanced for that of ΔE (500 rpm and 0.010 wt%). The arrows in the phase portraits indicate the direction of movement.

where Δf is the resonant-frequency shift due to the solution viscosity, f_0 the resonant fundamental frequency of the quartz crystal, μ the shear modulus of the quartz crystal and ρ the density of the quartz crystal. Equation (1) quantitatively explains the relationship between the resonant-frequency shift and the viscosity and density of a Newtonian liquid. From Fig. 2, the average amplitudes of ΔF of (a), (b), and (c) are 109, 40, and 57 Hz, respectively. Here, using Eq. 1, we attempted to convert ΔF into the concentration of sucrose at 20 °C, where the sucrose solution is known as the Newtonian liquid. This attempt revealed that ΔF = 109, 40, and 57 Hz corresponded to about 4, 1.5, and 2 wt%, respectively. The average periods of ΔF of (a), (b), and (c) are 24, 24, and 30 s, respectively. On the other hand, the average amplitudes of ΔE of (a), (b), and (c) are 15.5, 29.7, and 31.6 mV, respectively, and the average periods of ΔE are approximately the same as those of ΔF.

IV-2. Dynamical behavior of the phase difference between ΔE and ΔF of the BZ reaction

In the present paper, we are especially interested in the dynamical behavior of the phase difference between ΔE and ΔF of the BZ reaction. To investigate it, we systematically changed the stirrer bar speed and the solution viscosity and density. The results are indicated in Fig. 3. Figure 3 illustrates the region of the three types of the oscillation with the phase difference. Region-I means the region of the Type-I oscillation. The Type-I oscillation appears at the low speed of the stirrer bar over the present Triton X-100 concentration. On the other hand, the Type-III oscillation appears in Region-III. This area is wide and occupies the part of the high speed of the stirrer bar over the present Triton X-100 concentration. The Type-II oscillation is generated in the region between Region-I and Region-III. These results show that when the mixing level of the solution is low, the Type-I oscillation is dominant, and that when the mixing is high, the Type-III oscillation is lying above those for the other two types.

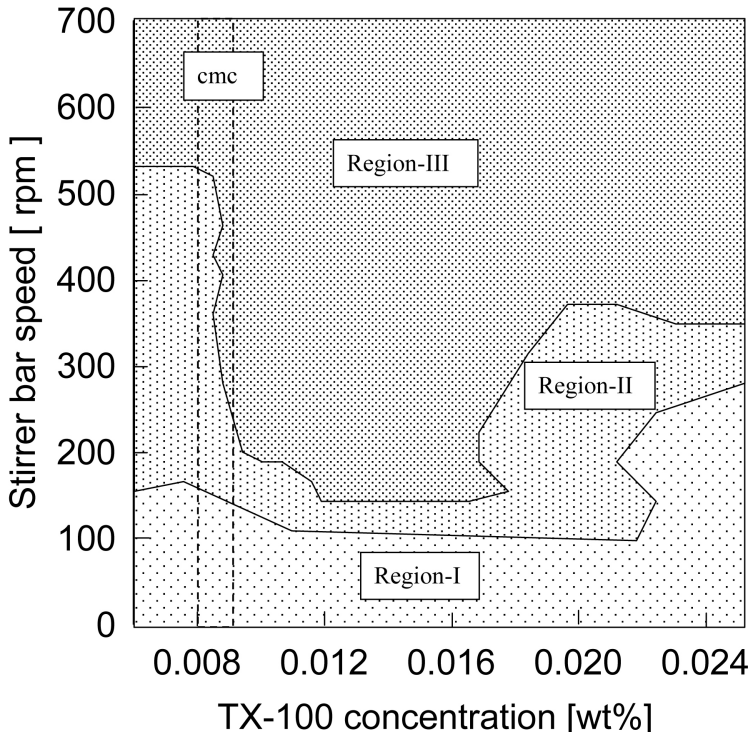

FIG. 3: Diagram of the phase difference between ΔE and ΔF of the BZ reaction. Region-I, Region-II, and Region-III show the regions of the oscillations of Type-I, Type-II, and Type-III, respectively. The region between the two dashed lines ($0.008 \sim 0.009$ wt%) shows the critical micellization concentration (cmc). The diagram is constructed from the average values calculated from 10 oscillations.

It is considered that the solution viscosity and density may be dependent on the degree of the decrease of the catalyst electrostriction and the number of the water molecules

rearranged due to the variation of the electric charge of the catalyst [13]. The oscillations of the Type-I and the Type-II oscillations are described by the above explanation. However, in the Type-III oscillation, the oscillation phase of ΔF comes before that of ΔE. It seems that this phenomenon is inconsistent with the previous description. However, the behavior of ΔE and ΔF in the critical micellization concentration (cmc) may give a clue. The cmc region is shown in Fig. 3, where the cmc was measured using the QCM. The boundary line between Region-II and Region-III changes drastically within the region of the cmc. On the other hand, the boundary line between Region-I and Region-II changes slightly. This phenomenon suggests that the cmc may play an important role in the oscillation of the solution viscosity and density. The micelle is formed above the cmc. This micelle may accelerate the Type-III oscillation by the interaction with the catalyst. The platinum electrode and the QCM measure the redox potential and the solution viscosity and density in the macro level, respectively. That is, the propagation speed from the molecular level to the macro level is very important in the measurement of the macro level of the redox potential and the solution viscosity and density. Above the cmc or at the high mixing level, the propagation speed of the solution viscosity and density may be advanced for that of the redox potential. On the other hand, at the low mixing level, the propagation speed of the redox potential may be advanced, because, at the low mixing level, the interactions between the catalyst, the micelle and the water become weak. Above 0.022wt% of the Triton X-100, the boundary line of Region-I increases again. This phenomenon indicates that the mixing effects may be weakened by the increase of the solution viscosity, and the propagation speed of the solution viscosity and density from the molecular level to the macro level may be retarded in that of the redox potential.

The above three types of phase lock synchronizations appear depending on the stirrer speed and the solution viscosity and density. Those phase lock synchronizations result in the deference of propagation speed from the molecular level to the macro level in the redox potential and the solution viscosity and density. In the next section we will make a study to obtain further insight into the mechanism of the behavior of the phase difference between ΔE and ΔF.

IV-3. Variation of the amplitudes of ΔE, ΔF and the oscillation period against the stirrer bar speed and the Triton X-100 concentration

Figure 4 shows the variation of the amplitudes of ΔE, ΔF and the oscillation period against the stirrer bar speed and the Triton X-100 concentration. The amplitudes of ΔF increase above the cmc and above 150 rpm of the stirrer bar speed (Fig. 4(a)). It is obvious that the cmc and the stirrer bar speed affect the oscillation of the solution viscosity and density. These results also suggest that the drastic variation of the amplitude of ΔF occurs in the region-II. On the other hand, at all stirrer bar speeds, the amplitudes of ΔE decrease with an increase in the Triton X-100 concentration (Fig. 4(b)). This phenomenon is the same as that reported by Paul [9]. The hydrodynamic character of the surfactant affects the amplitudes of ΔE. The oscillation periods increase with stirrer bar speed for all Triton X-100 concentrations (Fig. 4(c)). The tendency of this phenomenon is the same as that described by Menzinger and Jankowski [11]. This phenomenon is generated by the

homogenous intervention of the reactive gases.

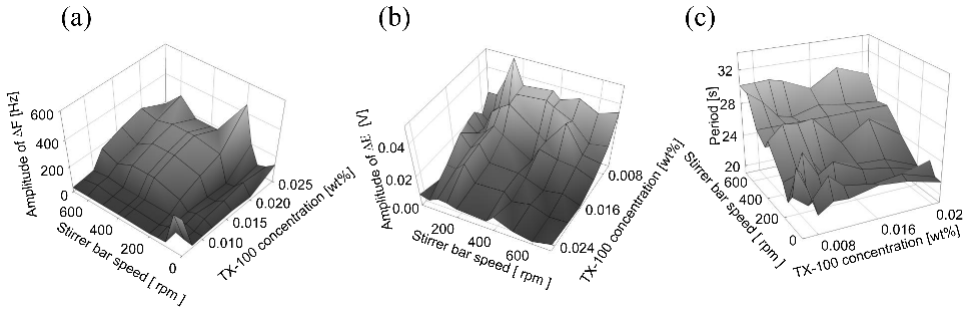

FIG. 4: Three-dimensional graphs of variation of the amplitudes and the periods of ΔE and ΔF. (a) The variation of the amplitude of ΔF. (b) The variation of the amplitude of ΔE. (c) The variation of periods of oscillations. We employ the average values calculated from 10 oscillations.

V. CONCLUSIONS

We have systematically investigated the dynamic behavior between the redox potential and the viscosity and density of the BZ reaction solution. This study has revealed that three types of oscillations with the phase difference appear depending on the stirrer bar speed and the solution viscosity and density. We have also found that the region of the existence of the Type-III oscillation is wide and appears at the high mixing levels, i.e., a homogenous solution.

The variation of the solution viscosity and density may be important in organisms. The cells of organisms have constantly an inflow and outflow of ions. The inflow and outflow of ions causes the variation of the intracellular quantity of the electric charge. Naturally, this phenomenon is accompanied with a variation of the solution viscosity and density within the cells. This change of the viscosity and density of the intracellular solution may affect the DNA control within the cells.

The chemical oscillation of the BZ reaction is converted into a variation of the viscosity and density of solution. In this paper, as the first step to create a model of chemomechanical coupling, we focused on the experimental study. We are now making a study to clarify the mechanism of the transformation of chemical reaction into the mechanical action.

References

[1] B. P. Belousov, Sb. Ref. Radiats. Med. **1**, 145 (1959).
[2] A. N. Zaikin and A. N. Zhabotinsky, Nature (London) **225**, 535 (1970). doi: 10.1038/225535b0
[3] S. K. Scott, Chemical *Chaos*, 1st ed. (Oxford University Press, Oxford, 1991).
[4] G. Bazsa and I. R. Epstein, J. Phys. Chem. **89**, 3050 (1985). doi: 10.1021/j100260a020

[5] H. Miike, S. C. Müller and B. Hess, Chem. Phys. Lett. **144**, 515 (1988). doi: 10.1016/0009-2614(88)87306-8
[6] J. A. Pojman and I. R. Epstein, J. Phys. Chem. **94**, 4966 (1990). doi: 10.1021/j100375a039
[7] N. Marchettini and M. Rustici, Chem. Phys. Lett. **317**, 647 (2000). doi: 10.1016/S0009-2614(99)01411-6
[8] M. Rustici *et al.*, Faraday Discuss. **120**, 39 (2001).
[9] A. Paul, J. Phys. Chem. B **109**, 9639 (2005). doi: 10.1021/jp044519j
[10] Y. Luo and I. R. Epstein, J. Chem. Phys. **85**, 5733 (1986). doi: 10.1063/1.451534
[11] M. Menzinger and P. Jankowski, J. Phys. Chem. **90**, 1217 (1986). doi: 10.1021/j100398a001
[12] F. Ali and M. Menzinger, J. Phys. Chem. **95**, 6408 (1991). doi: 10.1021/j100170a005
[13] M. Yoshimoto, H. Shirahama, S. Kurosawa, and M. Naito, J. Chem. Phys. **120**, 7067 (2004). doi: 10.1063/1.1676125
[14] K. K. Kanazawa and J. G. GordonII, Anal. Chim. Acta **175**, 99 (1985). doi: 10.1016/S0003-2670(00)82721-X
[15] D. A. Buttry and M. D. Ward, Chem. Rev. **92**, 1355 (1992). doi: 10.1021/cr00014a006
[16] F. Caruso, E. Rodda, and D. N. Furlong, J. Colloid Interface Sci. **178**, 104 (1996). doi: 10.1006/jcis.1996.0098
[17] H. M. Hastings *et al.*, J. Phys. Chem. A **112**, 4715 (2008). doi: 10.1021/jp8019073
[18] A. B. Rovindky and A. M. Zhabotinsky, J. Phys. Chem. **88**, 386 (1984). doi: 10.1021/j150645a002